Highly sensitive colorimetric detection of glucose in a serum based on DNA-embeded Au@Ag core–shell nanoparticles

2015 Nanotechnology 26 405707

(http://iopscience.iop.org/0957-4484/26/40/405707)

IOP Publishing Nanotechnology
Nanotechnology 26 (2015) 405707 (8pp) doi:10.1088/0957-4484/26/40/405707

Highly sensitive colorimetric detection of glucose in a serum based on DNA-embeded Au@Ag core–shell nanoparticles

Fei Kang[1], Xiangshu Hou[3] and Kun Xu[1,2]

[1] Department of Chemistry, University of Science and Technology of China, Hefei, Anhui 230026, People's Republic of China
[2] College of Chemistry and Pharmaceutical Engineering, Nanyang Normal University, Nanyang 473061, People's Republic of China
[3] The Hospital of University of Science and Technology of China, Hefei, Anhui 230026, People's Republic of China

E-mail: kunxu1@163.com

Received 8 July 2015
Accepted for publication 26 August 2015
Published 17 September 2015

Abstract

Glucose is a key energy substance in diverse biology and closely related to the life activities of the organism. To develop a simple and sensitive method for glucose detection is extremely urgent but still remains a key challenge. Herein, we report a colorimetric glucose sensor in a homogeneous system based on DNA-embedded core–shell Au@Ag nanoparticles. In this assay, a glucose substrate was first catalytically oxidized by glucose oxidase to produce H_2O_2 which would further oxidize and gradually etch the outer silver shell of Au@Ag nanoparticles. Afterwards, the solution color changed from yellow to red and the surface plasmon resonance (SPR) band of Au@Ag nanoparticles declined and red-shifted from 430 to 516 nm. Compared with previous silver-based glucose colorimetric detection strategies, the distinctive SPR band change is superior to the color variation, which is critical to the high sensitivity of this assay. Benefiting from the outstanding optical property, robust stability and well-dispersion of the core–shell Au@AgNPs hybrid, this colorimetric assay obtained a detection limit of glucose as low as 10 nM, which is at least a 10-fold improvement over other AgNPs-based procedures. Moreover, this optical biosensor was successfully employed to the determination of glucose in fetal bovine serum.

Keywords: glucose detection, Au@Ag nanoparticle, colorimetric assay

(Some figures may appear in colour only in the online journal)

1. Introduction

Glucose (monosaccharide) is a vital carbohydrate in biology that has been considered as a double-faced molecule due to its physiological and pathological effects. Furthermore, glucose is an important energy source for living cells and a metabolic intermediary, acting as a risk messenger in normal cellular signal transduction processes. As we all know, diabetes mellitus is a worldwide public health problem, and its complications, including higher risks of heart disease and kidney failure, have been identified as some of the leading causes of death in the world. All these symptoms can be reflected by abnormal blood glucose concentrations [1, 2]. It is therefore highly desirable to develop a simple biosensor platform to sensitively monitor the concentration of glucose on a daily basis [3–6].

Among many reported sensing methods, colorimetric biosensors have attracted much attention owing to their low cost, simplicity, practicality and unaided sophisticated instrumentation [7, 8]. In recent years, many nanoscale materials have been proven to function as a natural peroxidase mimic that can catalyze oxidation of 3, 3′, 5, 5-tetramethylbenzidine (TMB) by hydrogen peroxide to display a blue color. On the basis of this color change, these nanomaterials have emerged as a kind of colorimetric tool for the detection of glucose. Recently, it was reported that some

metal oxide nanomaterials such as Fe_3O_4 magnetic nanoparticles (NPs), CeO_2 NPs, CuO NPs, Co_3O_4 NPs and V_2O_5 nanowires possessed intrinsic peroxidase-like activity [9–14]. In addition, carbon nanomaterials with novel electronic, mechanical, and chemical properties, such as single-wall carbon nanotubes, carbon dots, graphene and graphene oxide (GO) [15–17] have been popular in constructing hybrid composite nanomaterials (PtNPs/GO, GO-COOH) for glucose detection [18, 19, 28]. In particular, these hybrid materials showed cooperatively enhanced performances for peroxidase-like catalysis [20–25].

Recently, silver nanoparticles (AgNPs) and graphene quantum dots (GQD)/AgNPs have been directly employed as optical glucose sensors on the basis of absorbance fading due to oxidation of Ag by H_2O_2 [26–28]. This oxidization process generated a sensitive color fading and can be used for colorimetric detection of glucose. In comparison with enzyme mimicking materials, silver nanomaterials show more superiorities: (1) Ag nanomaterials not only simplify the testing steps, but also decrease the cost [29, 30]. (2) The higher extinction coefficient of Ag NPs facilitates an increase in the slope of calibration curve and lead to a better sensitivity [31]. As we know, numerous attempts have been made to obtain steady AgNPs through surface modification with functional molecules, such as biological molecular, organic small molecular (poly (N-vinylpyrrolidone) (PVP)) and substituted phosphane ligands. However, it remains a great challenge to synthesize AgNPs with high dispersion, narrow and tunable size distribution [32–40]. Fortunately, DNA-functional nanotechnology and seed-assisted crystallization provide a new strategy to overcome these puzzles. Our group has previously developed a method to achieve reliable DNA-conjugated Au@Ag core–shell nanoparticles (Au@AgNPs) [41]. The existence of the gold core allowed us to control the structure, composition, and colloidal properties of the core–shell nanoparticles. In addition, the coating DNA on the gold cores gives the Au@AgNPs hybrids good stability and excellent salt resistance [41], which is beneficial for detection assays.

Herein, based on the outstanding properties of the DNA-embedded Au@Ag nanostructure [41], we proposed a facile and sensitive approach to colorimetrically detect glucose in water and fatal bovine serum (FBS). As shown in figure 1, the glucose substrate was first catalytically oxidized by glucose oxidase (GOx) to produce H_2O_2, then the *in situ* generated H_2O_2 could oxidize and etch the outer silver shell of Au@Ag nanoparticles in a homogeneous system, which resulted in the surface plasmon resonance (SPR) peak declining and red-shifting from 430 to 516 nm (characteristic absorption peak of Au@AgNPs and 5 nm AuNPs, respectively). The accompanying color variation from yellow to orange and then to red was sufficient for the naked eye to discern. Compared with previously reported colorimetric sensing based on silver materials, the two responsive phenomena including the SPR band decline and red-shift, and color change are superior to single color fading (e.g. ranges from yellow to pale), and are more sensitive for the naked eye. Benefiting from these outstanding optical properties, this approach achieves a low

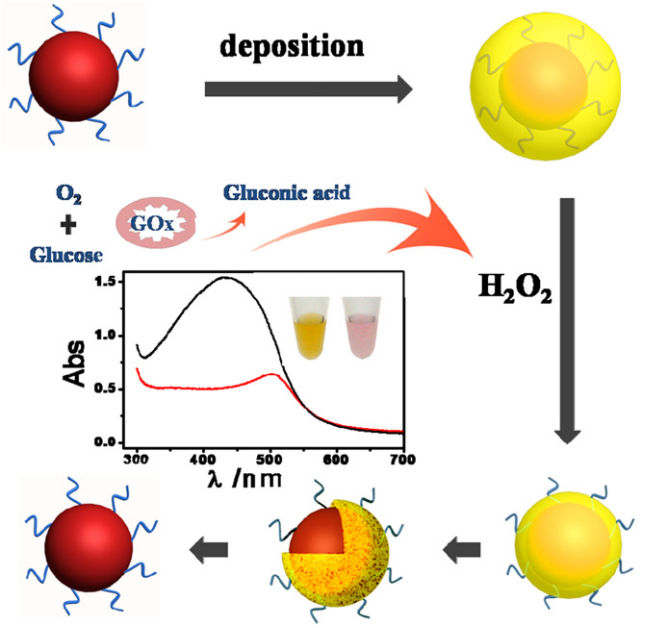

Figure 1. Schematic illustration of the glucose colorimetric detection sensor based on DNA-embedded Au@Ag nanoparticles.

detection limit for glucose as low as 10 nM and good linearity of the calibration curves at different glucose concentration regions (0–200 nM and 1–100 μM). Moreover, this nanocomposite is further extended to the glucose sensing in FBS and a detection value of 5.22 mM can be obtained.

2. Materials and methods

2.1. DNA sequences and chemicals

DNA oligonucleotides were custom-synthesized by Sangon Bioengineering Technology and Services Co., Ltd (Shanghai, China) and purified by PAGE (unmodified DNA) or HPLC (thiolated DNA).

dT10 strand (10 bases): HS-5′TTTTTTTTTT3′

Ascorbic acid (AA) and $AgNO_3$ were obtained from Bio Basic Inc. (BBI, Canada); polyvinylpyrro lidone (PVP K40, MW = 40 000), bis(p-sulfonatophenyl) phenylphosphine dihydrate dipotassium salt (BSPP) was a product of Strem Chemical (Newburyport, MA, USA). All the reagents were used as received without further purification. Glucose oxidase (GOx, 50 KU) was obtained from Sangon Bioengineering Technology and Services Co., Ltd (Shanghai, China). Fetal bovine serum (FBS) was obtained from Zhejiang Tianhang Biotechnology Co., Ltd (China). Glucose, D-fructose, α-lactose, sucrose and maltose were purchased from Sinopharm Chemical Reagent Co., Ltd.

2.2. Synthesis of DNA-embedded Au@AgNPs

Firstly, 5 nm Au nanoparticles were prepared according to a published method [42]. Then, the 5'-thiolated dT10 strand was combined with 1 μM 5 nm AuNPs at a 60:1 molar ratio and the mixture was incubated in 0.5 × TBE buffer (Tris,

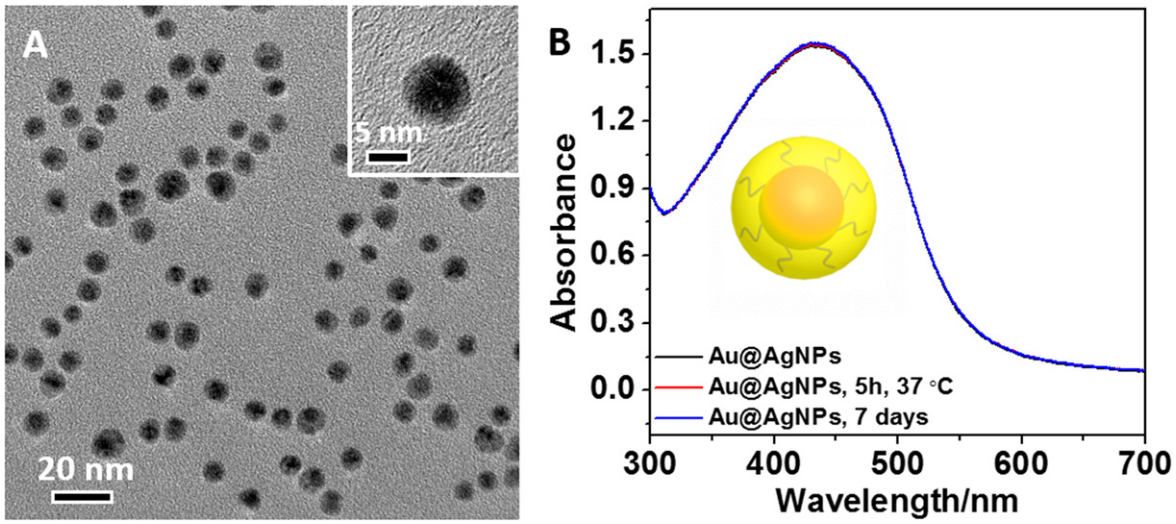

Figure 2. (A) TEM image of Au@AgNPs; inset is the high-magnification TEM image; (B) UV–vis spectra of Au@AgNPs after treated with different temperatures and storage time.

44.5 mM; EDTA, 1 mM; boric acid, 44.5 mM; pH 8.0) and 100 mM NaCl at 20 °C for 3 h. Later, 30 μL of the resulting dT10-modified AuNPs at a concentration of 1 μM were mixed with 6 μL 40 mM $AgNO_3$, 6 μL 100 mM ascorbic acid, and 1.5 μL 10% PVP in 0.5 × TBE plus 0.1 M NaCl. The reaction lasted for 3 h at room temperature. After centrifugation at 13 000 rpm for 40 min, concentrated Au@AgNPs was obtained and stored for further use.

2.3. Colorimetric assay for glucose

Before testing, we scrutinized the effects of glucose oxide concentration (GOx, 6, 8, 10, 12, 14 U) and reaction time on the absorbance. Detection of glucose in the buffer was performed in the following steps: (1) different concentrations of glucose (from 0.01 to 200 μM) were respectively incubated with glucose oxidase (GOx, 100 μg mL^{-1}) in 100 μL HAc-NaAc buffer (pH = 4.5, 20 mM) at 37 °C for 30 min; (2) after incubation, 5 μL 200 mM NaOH was added into the solution to keep the pH at 8.0. Then 1.5 μL of above the Au@AgNPs were introduced into the solution. The photograph (against white light) and UV–vis absorbance spectrum after 2 h was measured. (3) For the selectivity test, 5 mM of fructose, galactose, and sucrose were incubated with GOx respectively in the same way.

2.4. For sensing glucose in FBS and interference testing

For glucose detection in the real FBS sample, the standard addition method was used. Glucose was added into FBS with varying concentrations (25−200 nM). Then, 1 μL of 1000 times diluted FBS with or without glucose addition was added into the buffer. The calculated value was multiplied by 400 000 to obtain the glucose concentration in serum. The Dimension RxL Max integrated chemistry system (Siemens Company) was used as a standard method to determine the concentration of glucose in undiluted serum. For the interference experiment in the FBS, some present metal ions, amino acid and proteins including Na^+, Mg^{2+}, Ca^{2+}, Fe^{3+}, bovine serum albumin (BSA), cysteine (Cys), histidine (His) and glycine (Gly) were tested to evaluate the selectivity of the assay. The concentration of all the interference reagents was 5 mM, which was 25 times more than FBS. The concentration of FBS in the interference testing was diluted by approximately 20 times.

2.5. UV–vis spectroscopy and TEM characterizations

UV–vis spectra for a series of samples were recorded by a UV-3600 Shimadzu UV–vis-NIR spectrophotometer. For transmission electron microscope (TEM) analysis, 5 μL samples including Au@AgNPs in the absence of and presence of glucose were respectively deposited on a carbon-coated copper grid (200 mesh) under ambient conditions. TEM imaging was conducted on a JEM-2100F field emission transmission electron microscope operated at an acceleration voltage of 200 kV.

3. Results and discussion

3.1. Characterization of Au@AgNPs

The morphology and size of the as-prepared Au@AgNPs were characterized by TEM, and the result revealed the core–shell nanostructure of Au@AgNPs with an average diameter about 9 nm. As illustrated in figure 2(A), the high resolution TEM (HR-TEM) image revealed a shell thickness of about 3 nm. As shown in figure 2(B), the constant plasmonic absorbance of Au@AgNPs implied their outstanding stability at different temperatures and storage times, which is due to the highly charged DNA acting as a capping agent and making the AuNPs-core surface with highly coulombic repulsions during the nucleation process [39, 40]. The characteristic plasmonic absorption peak at 430 nm suggested successful silver shell deposition on the Au core, and the

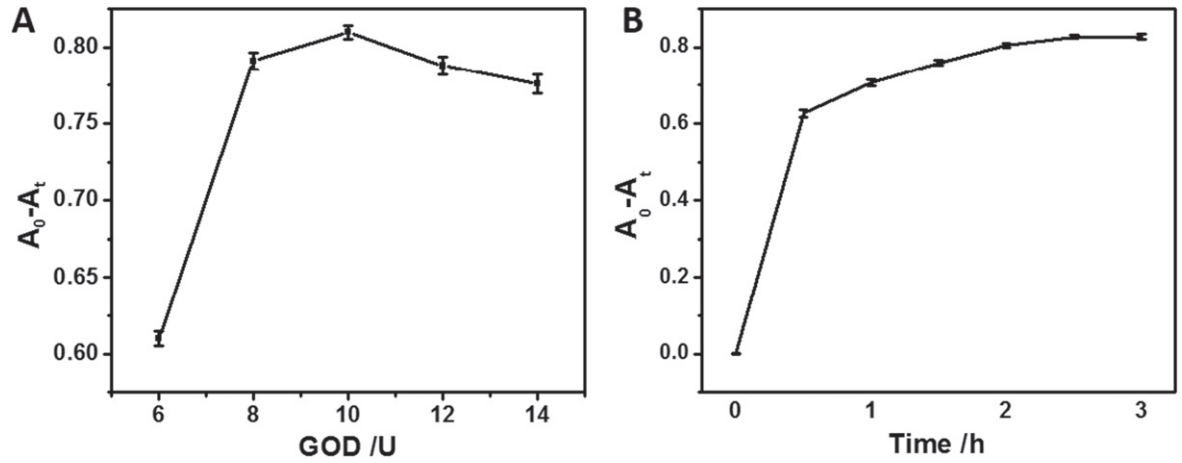

Figure 3. The effects of GOx concentrations (A) and reaction time (B) on the A_0–A_t absorbance.

Au@AgNPs solution appeared to be a yellow color which is close to that of AgNPs. In contrast, Au@AgNPs in the absence of dT10 exhibited a poor dimensional homogeneity and dispersion, as shown in gel electrophoretograms; UV–vis absorption spectra and TEM images are shown in figures S1 and S2 in the supporting information. TEM images of Au@AgNPs stored for at least one week are also shown in figure S3, which once again proved the highly stability of DNA-embedded Au@AgNPs.

3.2. Optimization of experimental conditions

In order to achieve the optimal performance for glucose detection, the effects of glucose oxide (GOx) concentration and reaction time on the absorbance have been investigated. Because the reaction rate depended on the enzyme concentration, the absorption value variation reached its maximum at 10 U enzyme activity, as exhibited in figure 3(A). Interestingly, In figure 3(B), the absorbance value changed sharply within the first 40 min, but the A_0–A_t (A_0, A_t corresponds to the maximum absorbance value at initial and end time respectively) absorbance did not reach stabilization until approximately 2 h later. No further change in the SPR band was observed through the solution. We deduced that in this system the cascade reactions involving glucose, GOx, gluconic acid, H_2O_2, and H^+ would need a certain amount of time to achieve a balance [43]. Thus, we chose 10 U GOx and two hours reaction time as the optimal reaction conditions in the following experiments.

3.3. Colorimetric detection of glucose.

It is reported that glucose oxidase (GOx) can specifically catalyze the oxidation of glucose in the presence of oxygen to generate H_2O_2 [45]. Figure 4(A) illustrates that after treating with different concentrations of glucose (from left to right were 0.0, 0.5, 10, 30, 50, 100, 200 μM), Au@AgNPs solution color exhibited a transition from yellow to orange and then to red. In comparison with many glucose colorimetric biosensors ranging from yellow to pale, the color variation interval was relatively wide, which is more likely to be discerned. Figure 4(B) presented the UV–vis absorption spectra of the Au@AgNPs solution with and without various amounts of glucose (0.01–200 μM). The surface plasmon resonance (SPR) band of the Au@AgNPs sample decreased and shifted to longer wavelengths (from 430 to 516 nm), consistent with the observed color change from yellow to red. That was due to the H_2O_2 generated in GOx catalytically oxidation of glucose could oxidize the silver shell of core–shell Au@Ag nanoparticles ($Ag^0 + H_2O_2 \rightarrow Ag^+ + O_2^{\bullet -} + 2H_2O$) [28], and then the inner gold cores were gradually uncovered, resulting in the SPR bands of Au@AgNPs solution declining and red-shifting from 430 to 516 nm. Compared with previously reported colorimetric sensors based on silver nanomaterials [26–28], the two phenomena including the SPR peak intensity decline and red-shift were superior to color transition changes, and were more sensitive to the naked eye. This observation provides great potential for quantitative detection of glucose.

As shown in figure 4(C), a series of changes were achieved by plotting A_0−A_t versus glucose concentrations within a range of 0.00 μM to 200 μM. In comparison with some previously reported colorimetric procedures for glucose detection [26–28], this colorimetric approach achieved a detection limit of glucose at 0.01 μM, which is at least a 10-fold improvement over other AgNPs-based procedures (see table 1). After optimizing the experimental parameters, two linear calibration curves were obtained by plotting the absorbance change versus glucose concentration within 0.00–0.20 and 1.00–100 μM ($R^2 = 0.994$ and $R^2 = 0.996$, respectively), as shown in figures 4(D) and (E). With respect to the mutational site in the two calibration curves, a possible explanation has been given in previously reported work [44]. We concluded that when the concentration of glucose was high, a large amount of generated sodium gluconate may have reacted with Au@AgNPs and then decreased the reaction ability of hydrogen peroxide with the nanoparticles, leading to a low absorbance decreasing efficiency. Benefiting from the above two linear ranges, we were able achieve quantitative glucose detection both at low and high concentration ranges.

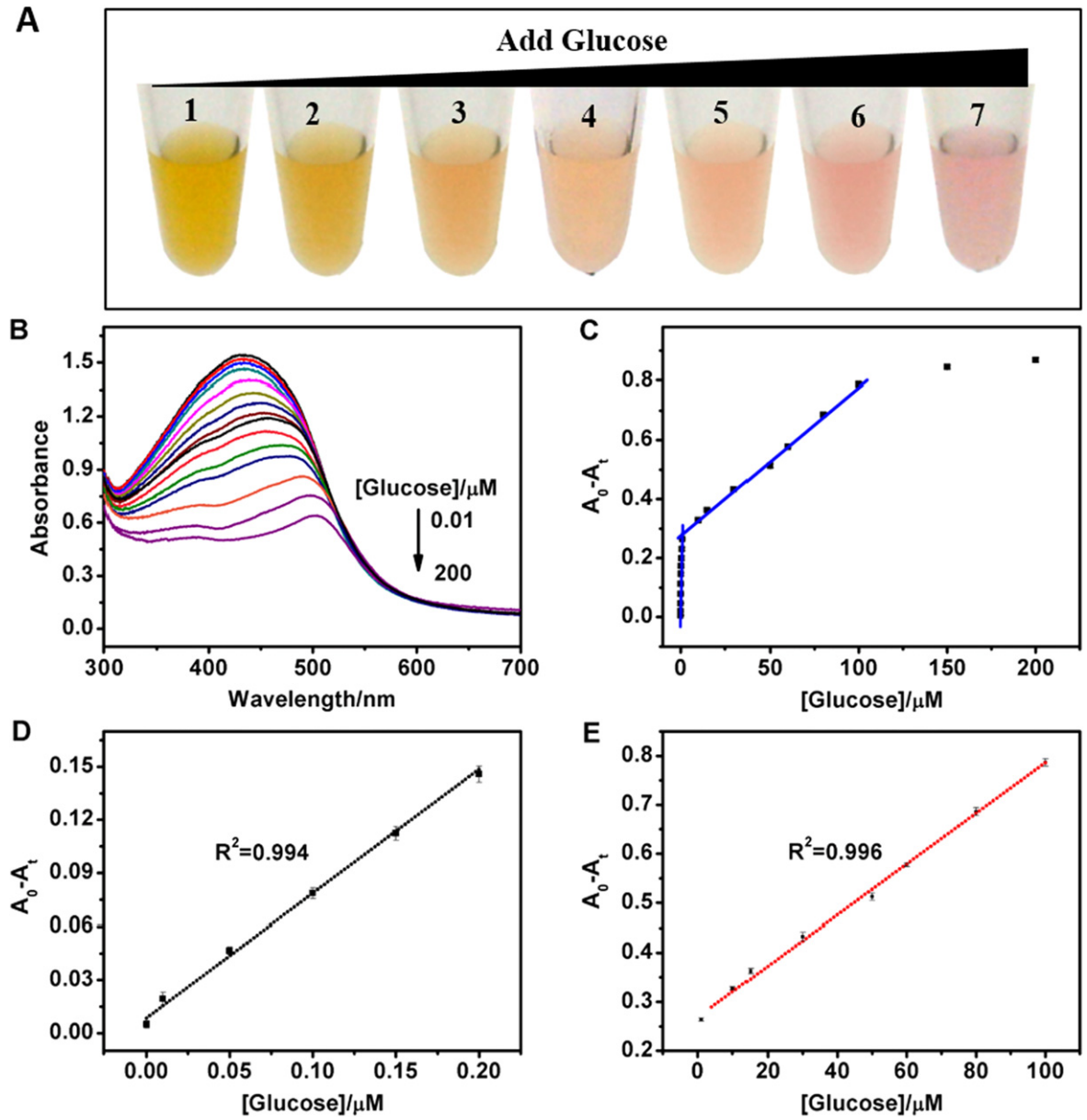

Figure 4. (A) Photographs of Au@AgNPs solution in the presence of 0.0, 0.5, 10, 30, 50, 100 and 200 μM glucose; (B) UV–vis absorption spectra of Au@AgNPs samples treated without and with different concentrations of glucose from 0.01 μM to 200 μM; (C) absorption value change of Au@AgNPs in the presence of 0.0, 0.01, 0.05, 0.10, 0.20, 0.50, 1.00, 10.0, 15.0, 30.0, 50.0, 60.0, 80.0, 100 and 200 μM glucose; two linear calibration graphs by plotting the absorbance change versus glucose concentration within (D) 0.00—0.20 μM and (E)1.0—100 μM.

The morphologies of Au@AgNPs after treatment with 200 μM glucose and GOx were characterized by TEM (figure 5(A)). As can be seen from the TEM image, the inner gold cores were exposed with a good dispersion, indicating that the silver shell has been completely oxidized and etched. However, at a low glucose concentration, some Ag shells failed to be etched because the generated H_2O_2 by catalytic reaction was insufficient, as can be seen in figure S4. Figure 5(B) presented the selectivity test of Au@AgNPs sample towards 200 μM glucose and other carbohydrates at a concentration of 5 mM, including D-fructose, α-lactose, sucrose and maltose. However, other saccharides exhibited nearly no response to the Au@AgNPs sample, which indicated that the Au@AgNPs-based detection system possessed a specific response to glucose (~25 times more sensitive than other carbohydrates). The excellent selectivity and low detection limit of this assay, as well as good stability of Au@AgNPs, provide great potential for practical applications.

3.4. Detection of glucose in FBS and interference testing

The first linear calibration and standard addition method were used to detect glucose in real samples as the standard curve would pass the zero point. The high dilution ratio can minimize the influence of the matrix effect for complex samples.

Table 1 Performances of various glucose sensors.

Biosensing materials	Analytical method	LOD (μM)	Linear range (μM)	Reference
G-AgNPs	Electrochemistry	100	2000–10 000	[49]
GO-AgNPs	Electrochemistry	310	2000–12 000	[50]
rGO-AgNPs[a]	Electrochemistry	4.5	32–1890	[51]
PEI-AgNCs[b]	Fluorimetry	0.8	1–10, 10–1000	[44]
CeO_2NPs	Fluorimetry	8.9	10–200	[10]
Ch-AgNPs[c]	Colorimetry	0.1	5–200	[27]
GQDs/AgNPs	Colorimetry	0.17	0.5–400	[28]
AgNPs	Colorimetry	130	270–4440	[26]
Au@AgNPs	Colorimetry	0.01	0.01–0.2, 1–100	This work

[a] rGO: reduced graphene oxide;
[b] PEI-AgNCs: polyethyleneimine-capped silver nanoclusters;
[c] Ch-AgNPs: chitosan stabilized silver nanoparticles G: graphene,

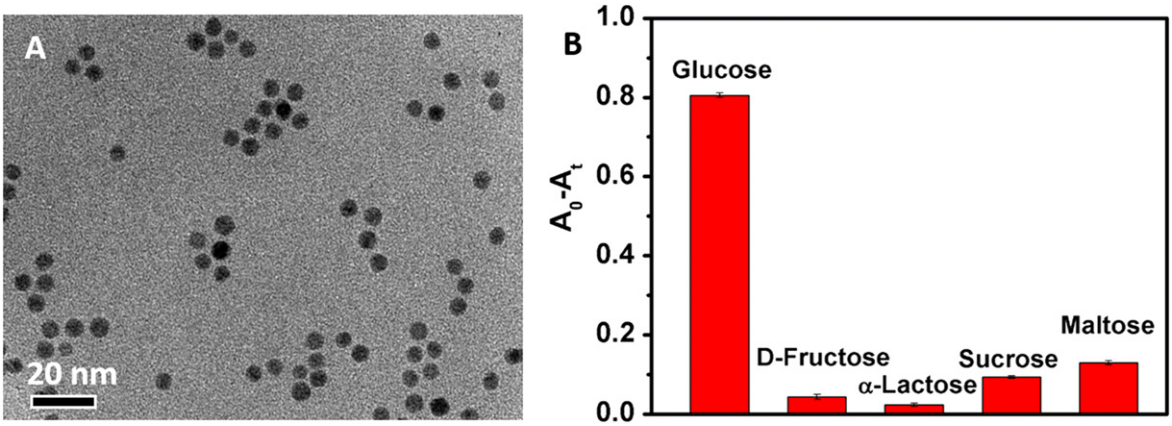

Figure 5. (A) TEM images of Au@AgNPs after treated with 200 μM glucose and GOx; (B) sensor selectivity test of Au@AgNPs in the presence of 200 μM glucose and other carbohydrates at a concentration of 5 mM.

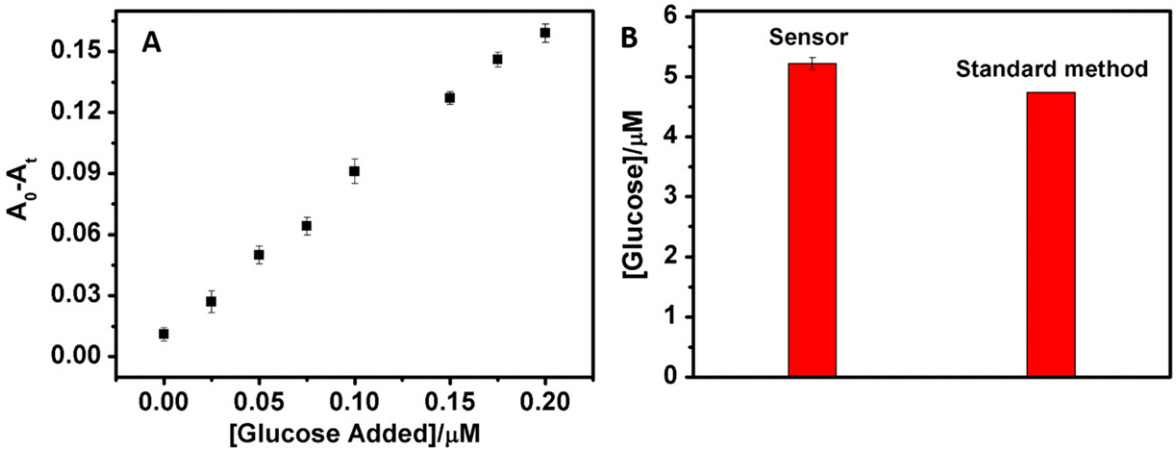

Figure 6. (A) The standard addition method of glucose into serum sample to determine the glucose concentration using a Au@AgNPs-based sensor; (B) comparison between glucose detection in serum by Au@AgNPs-based sensor and the standard method by Dimension RxL Max integrated chemistry system (Siemens Company).

For sensing glucose in FBS, glucose was added into the FBS with different concentrations (0.025–0.20 μM). As shown in figure 6(A), a value of approximately 5.22 mM of glucose in FBS was obtained by standard addition method calculation. A standard method by Dimension RxL Max integrated chemistry system (Siemens Company) was also used to determine the concentration of glucose in undiluted serum and a value of 4.74 mM was obtained. The results provided by our proposed method are close to the values determined by the large precision instrument testing (in figure 6(B)), indicating this Au@AgNPs-based sensor is compatible in a complex sample matrix.

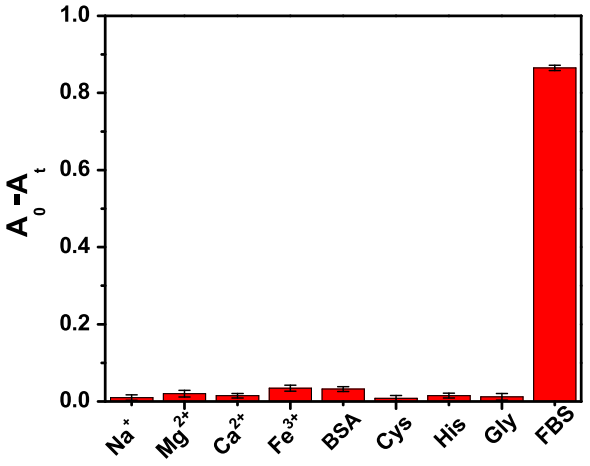

Figure 7. Sensor for potential biochemical interference test in the presence of FBS diluted by 20 times and other potential existing biochemicals including metal ions, BSA, Cys, His and Gly with a concentration of 5 mM.

Due to the real sample possessing a complicated environmental system, some potential existing biochemicals including metal ions (Na^+, Mg^{2+}, Ca^{2+}, Fe^{3+}), bovine serum albumin (BSA), cysteine (Cys), histidine (His) and glycine (Gly) were tested to evaluate the selectivity of the assay with the determination of FBS in this study[46–48], as shown in figure 7. The results confirmed that our system has a high selectivity for glucose even in the presence of other interfering agents. As we know, selectivity for the real sample plays a significant role in estimating the performance of a new biosensor.

4. Conclusions

In summary, we developed a highly sensitive method for colorimetric glucose detection by using DNA-embedded Au@Ag core–shell nanoparticles as substrates. In this assay, a glucose substrate was first catalytically oxidized by glucose oxidase to produce H_2O_2 which would further oxidize and gradually etch the outer silver shell of Au@Ag nanoparticles. As a result, the solution color changed from yellow to red and the surface plasmon resonance (SPR) band of Au@Ag nanoparticles declined and red-shifted from 430 to 516 nm. Compared with previously reported silver-based colorimetric sensors, the present two distinct phenomena were more inclined to be recognized by the naked eye. This colorimetric approach achieved a sensitive detection limit of glucose as low as 10 nM, which is at least a 10-fold improvement in the sensitivity over other AgNPs-based procedures. Owing to the excellent stability and low detection limit, this optical biosensor was further successfully employed to determine glucose in fetal bovine serum, the results of which was close to the standard method.

Acknowledgments

The authors are thankful to the hospital of University Science and technology of China for providing the FBS test.

References

[1] Wang J 2008 Electrochemical glucose biosensors *Chem. Rev.* **108** 814–25
[2] Giorgio M, Trinei M, Migliaccio E and Pelicci P G 2007 Hydrogen peroxide: a metabolic by-product or a common mediator of ageing signals *Nat. Rev. Mol. Cell Biol.* **8** 722–8
[3] Reach G and Wilson G S 1992 Can continuous glucose monitoring be used for the treatment of diabetes *Anal. Chem.* **64** 381A–6A
[4] Wang J 2001 Glucose biosensors: 40 years of advances and challenges *Electroanalysis* **13** 983–8
[5] Gomes A, Fernandes E and Lima J L F C 2005 Fluorescence probes used for detection of reactive oxygen species *J. Biochem. Biophys. Methods* **65** 45–80
[6] Chen X Q, Tian X Z, Shin I and Yoon J 2011 Fluorescent and luminescent probes for detection of reactive oxygen andnitrogen species *Chem. Soc. Rev.* **40** 4783–804
[7] Song Y J, Wei W L and Qu X G 2011 Colorimetric biosensing using smart materials *Adv. Mater.* **23** 4215–36
[8] Song S, Qin Y, He Y, Huang Q, Fan C and Chen H Y 2010 Functional nanoprobesfor ultrasensitive detection of biomolecules *Chem. Soc. Rev.* **39** 4234–43
[9] Gao L Z *et al* 2007 Intrinsic peroxidase-like activity of ferromagnetic nanoparticles *Nat. Nanotechnology* **2** 577–83
[10] Liu B, Sun Z Y, Huang P J J and Liu J W 2015 Hydrogen peroxide displacing DNA from nanoceria: mechanism and detection of glucose in serum *J. Am. Chem. Soc.* **137** 1290–5
[11] Asati A, Santra S, Kaittanis C, Nath S and Perez J M 2009 Oxidase-like activity of polymer-coated cerium oxide nanoparticles *Angew. Chem., Int. Ed.* **48** 2308–12
[12] Chen W, Chen J, Liu A L, Wang L M, Li G W and Lin X H 2011 Peroxidase-like activity of cupric oxide nanoparticle *Chem. Cat. Chem.* **3** 1151–4
[13] Mu J, Wang Y, Zhao M and Zhang L 2012 Intrinsic peroxidase-like activity and catalase-like activity of Co_3O_4 nanoparticles *Chem. Commun.* **48** 2540–2
[14] Andre R, Natalio F, Humanes M, Leppin J, Heinze K, Wever R, Schroeder H C, Mueller W E G and Tremel W 2011 V_2O_5 nanowires with an intrinsic peroxidase-like activity *Adv. Funct. Mater.* **21** 501–9
[15] Li X L, Wang X R, Zhang L, Lee S W and Dai H J 2008 Highly conducting graphene sheets and Langmuir-Blodgett films *Science* **319** 1229–32
[16] Wang X H, Wang C Y, Qu K G, Song Y J, Ren J S, Miyoshi D, Sugimoto N and Qu X G 2010 Ultrasensitive and selective detection of a prognostic indicator in early-stage cancer using graphene oxide and carbon nanotubes *Adv. Funct. Mater.* **20** 3967–71
[17] Liu Z, Robinson J T, Sun X M and Dai H J 2008 PEGylated nano-graphene oxide for delivery of water insoluble cancer drugs *J. Am. Chem. Soc.* **130** 10876–7
[18] Na Z L, Deng H H, Lin F L, Xu X W, Weng S H, Liu A L, Lin X H, Xia X H and Chen W 2014 In situ growth of porous platinum nanoparticles on graphene oxide for colorimetric detection of cancer cells *Anal. Chem.* **86** 2711–8
[19] Song Y J, Qu K G, Zhao C, Ren J S and Qu X G 2010 Graphene oxide: intrinsic peroxidase catalytic activity and its application to glucose detection *Adv. Mater.* **22** 2206–10
[20] He X L, Tan L F, Chen D, Wu X L, Ren X L, Zhang Y Q, Meng X W and Tang F Q 2013 Fe_3O_4–Au@mesoporous SiO_2 microspheres: an ideal artificial enzymatic cascade system *Chem. Commun.* **49** 4643–5
[21] Liu S, Tian J Q, Wang L, Luo Y L, Chang G H and Sun X P 2011 Iron-substituted SBA-15 microparticles: a peroxidase-like catalyst for H_2O_2 detection *Analyst* **136** 4894–7

[22] Guo Y J, Deng L, Li J, Guo S J, Wang E K and Dong S J 2011 Hemin−graphene hybrid nanosheets with intrinsic peroxidase-like activity for label-free colorimetric detection of single-nucleotide polymorphism *ACS Nano* **5** 1282–90

[23] Hao J H, Zhang Z, Yang W S, Lu B P, Ke X, Zhang B L and Tang J L 2013 *In situ* controllable growth of $CoFe_2O_4$ ferrite nanocubes on graphene for colorimetric detection of hydrogen peroxide *J. Mater. Chem.* A **1** 4352–7

[24] Lee Y M, Garcia M A, Huls N A F and Sun S H 2010 Synthetic tuning of catalytic properties of Au-Fe_3O_4 nanoparticles *Angew. Chem., Int. Ed.* **49** 1271–4

[25] Liu M, Zhao H M, Chen S, Yu H T and Quan X 2012 Interface engineering catalytic graphene for smart colorimetric biosensing *ACS Nano* **6** 3142–51

[26] Tashkhourian J, Hormozi-Nezhad M R, Khodaveisi J and Dashti R 2011 A novel photometric glucose biosensor based on decolorizing of silver nanoparticles *Sensors Actuators* B **158** 185–9

[27] Jiang H, Chen Z H, Cao H Y and Huang Y M 2012 Peroxidase-like activity of chitosan stabilized silver nanoparticles for visual and colorimetric detection of glucose *Analyst* **137** 5560–4

[28] Chen S, Hai X, Chen X W and Wang J H 2014 In situ growth of silver nanoparticles on graphene quantum dots for ultrasensitive colorimetric detection of H_2O_2 and glucose *Anal. Chem.* **86** 6689–94

[29] Lee J S, Lytton-Jean A K R, Hurst S J and Mirkin C A 2007 Silver nanoparticle oligonucleotide conjugates based on DNA with triple cyclic disulfide moieties *Nano Lett.* **7** 2112–5

[30] Chernousova S and Epple M 2013 Silver as antibacterial agent: ion, nanoparticle, and metal *Angew. Chem., Int. Ed.* **52** 1636–53

[31] Murphy C J *et al* 2008 Chemical sensing and imaging with metallic nanorods *Chem. Commun.* 5544–7

[32] Chen Y, Aveyard J and Wilson R 2004 Gold and silver nanoparticles functionalized with known numbers of oligonucleotides per particle for DNA detection *Chem. Commun.* **24** 2804–5

[33] Li H, Cui Z M and Han C P 2009 Glutathione-stabilized silver nanoparticles as colorimetric sensor for Ni^{2+} ion *Sensors Actuators* B **143** 87–92

[34] Chen Z, Luo Y, He S, Lin H, Chen Y, Sheng P, Li J, Chen B, Liu C and Cai Q 2010 Simple and sensitive colorimetric detection of cysteine based on ssDNA-stabilized gold nanoparticles *Analyst* **135** 1066–9

[35] Zhang M and Ye B C 2011 Colorimetric chiral recognition of enantiomers using the nucleotide-capped silver nanoparticles *Anal. Chem.* **83** 1504–9

[36] Ma Y, Niu H, Zhang X and Cai Y 2011 One-step synthesis of silver/dopamine nanoparticles and visual detection of melamine in raw milk *Analyst* **136** 4192–6

[37] Xiong D, Chen M and Li H 2008 Synthesis of *para*-sulfonatocalix[4]arene-modified silver nanoparticles as colorimetric histidine probes *Chem. Commun.* **7** 880–2

[38] Kittler S *et al* 2010 The influence of proteins on the dispersability and cell-biological activity of silver nanoparticles *J. Mater. Chem.* **20** 512–8

[39] Zheng Y Q, Li Y L and Deng Z X 2012 Silver-nanoparticle-DNA bionanoconjugates bearing a discrete number of DNA ligands *Chem. Commun.* **48** 6160–2

[40] Li Y L, Zheng Y Q, Gong M and Deng Z X 2012 Pt nanoparticles decorated with a discrete number of DNA molecules for programmable assembly of Au/Pt bimetallic superstructures *Chem. Commun.* **48** 3727–9

[41] Wang H Q, Li Y L, Gong M and Deng Z X 2014 Core solution: a strategy towards gold core/non-gold shell nanoparticles bearing strict DNA-valences for programmable nanoassembly *Chem. Sci.* **5** 1015–20

[42] Slot J W and Geuze H J 1985 A new method of preparing gold probes for multiple-labeling cytochemistry *Eur. J. Cell. Biol.* **38** 87–93

[43] Le X *et al* 2014 Fibrous nano-silica containing immobilized Ni@Au core–shell nanoparticles: a highly active and reusable catalyst for the reduction of 4-nitrophenol and 2-nitroaniline *J. Mol. Catal.* A **395** 58–65

[44] Wen T, Qu F, Li N B and Luo H Q 2012 Polyethyleneimine-capped silver nanoclusters as a fluorescence probe for sensitive detection of hydrogen peroxide and glucose *Anal. Chim. Acta.* **749** 56–62

[45] Refaey S A M 2000 Inhibition of chloride pitting corrosion of mild steel by sodium gluconate *Appl. Surf. Sci.* **157** 199–206

[46] Yokus B *et al* 2006 Effects of seasonal and physiological variations on the serum chemistry, vitamins and thyroid hormone concentrations in sheep *J. Vet. Med. Ser.* A **53** 271–6

[47] Xian Y *et al* 2013 An ultrasensitive, non-enzymatic glucose assay via gold nanorod-assisted generation of silver nanoparticles *Nanoscale* **5** 6303–6

[48] Cao K *et al* 2014 Phenylboronic acid modified silver nanoparticles for colorimetric dynamic analysis of glucose *Biosens. Bioelectron.* **52** 188–95

[49] Zhang Y, Liu S, Wang L, Qin X, Tian J, Lu W, Chang G and Sun X 2012 One-pot green synthesis of Ag nanoparticles-graphene nanocomposites and their applications in SERS, H_2O_2, and glucose sensing *RSC Adv.* **2** 538–45

[50] Lu W, Luo Y, Chang G and Sun X 2011 Synthesis of functional SiO_2-coated graphene oxide nanosheets decorated with Ag nanoparticles for H_2O_2 and glucose detection *Biosens. Bioelectron.* **26** 4791–7

[51] Luo Z, Yuwen L, Han Y, Tian J, Zhu X, Weng L and Wang L 2012 Reduced graphene oxide/PAMAM–silver nanoparticles nanocomposite modified electrode for direct electrochemistry of glucose oxidase and glucose sensing *Biosens. Bioelectron.* **36** 179–85